Basrah Journal for Engineering Sciences, Vol. 21, No. 1, (2021), 38-49

Original Article

Journal homepage: www.bjes.edu.iq
ISSN (Online): 23118385, ISSN (Print): 18146120

OPEN ACCESS

Detecting Vibration Problems in Machines and Structures Using Motion Capturing by Camera

Husam Sattar Jasim [1,*], Jaafar Khalaf Ali [2]

[1,2] *Department of Mechanical Engineering, College of Engineering, University of Basrah, Basrah, Iraq*
E-mail addresses: husamsattar91@gmail.com , jaafarkhalaf@yahoo.com
Received: 3 October 2020; Revised: 24 October 2020; Accepted: 28 October 2020; Published: 17 January 2021

Abstract

Vibration in rotating machines and structures is normally measured using accelerometers and other vibration sensors. For large machines and structures, the process of collecting vibration data is tedious and time-consuming due to the large number of points where vibration data must be measured. In this paper, a novel non-contact vibration measurement method has been introduced by using a high-speed camera as a vibration measurement device. This method has many advantages compared with the others. It has a low cost, easy to setup, and high automation. It also can be used for full-field measurement. Many tests have been accomplished to prove the validation of this method. The verification test has been accomplished by using the machinery faults simulator. It presented a reasonable validation that the operation deflection shapes (ODS) and the phase difference of any object can be successfully measured by using a high-speed camera. The mode shape tests have been accomplished by using the whirling of shaft apparatus device to extract the time domain, frequency domain, ODS, and phase differences for many points on the shaft at the first two critical speeds. The results proved that the high-speed camera can be used to detect the vibration signal in many different fault cases. It also proved that the high-speed camera can be used to detect the ODS and the phase angle difference. That gives the proposed method more robust and acceptance.

Keywords: Non-contact vibration measurement, high-speed camera, operation deflection shapes, phase angle difference.

https://doi.org/10.33971/bjes.21.1.6

1. Introduction

Vibration detection and analysis are very important in the maintenance engineering field. It's continuously developing and still a big challenge to introduce new methods in the field of the vibration measurement system with increasing adaptability, high automation, and high accuracy. It can be classifying the vibration measurement technology into two groups: contacting measurements and non-contacting measurements. In contacting measurements, the measuring sensor is attached to a body in motion directly according to a certain mechanism and connected with the processing system, such as accelerometers and LVDT displacement sensors, etc.

The contact type methods may not be practical for some large structures, the handling of all the measurement devices and their accessories needs to long time and very big effort. Another disadvantage of the contacting measurement is the mass loading effects [1]. This phenomenon occurs when it needs to measure the vibration of lightweight structures, that make the reading data sensitive for the weight of the used sensor.

The other type of vibration measurement is the non-contacting measurements. The use of this type eliminates any chance of whether mass loading effects are disturbing vibration data or not, because of that there is no contacting between the sensor and the body in motion. There are a lot of non-contacting measurement types, for example, the laser Doppler Vibrometer (LDV). In the last years, new non-contacting measurements have been proposed. It uses computer vision techniques to extract the vibration information from videos. One of these types is the digital camera. It can be used to extract the displacements of structures. By making a comparison with the Laser Doppler Vibrometer (LDV), the advantages of using the digital cameras are:

- Low cost.
- Easy to setup.
- High automation.
- Can be used for full-field measurement.

In the last years, camera vision-based measurement methods had been developed. The 3D digital image correlation method (3D DIC) is one of the camera vision-based measurement methods, it's used widely in the previous works. The development of the (3D DIC) technique leads to use it to measure the deformation of shapes and vibration of the structures. The technique allows for full-field measurement of structural response.

Helfrick et al. [2] proposed a related work to (3D-DIC). This work presented some primary results for the test, analysis, and correlation of vibration data which measured using the (3D DIC) method with traditional accelerometers and a scanning laser vibrometer for comparing with a finite element model. The results show that all three methods have a good correlation with the finite element model and provide validation for the (3D DIC) method for vibration measurement.

Optical flow is another method of camera vision-based measurement method. It depends on image intensity information (Intensity-based). It's proposed at first by Horn and Schunck [3]. They presented a method to find the optical flow pattern which supposed that the apparent velocity of the brightness pattern changes smoothly at any point in the image. In [3], they show a repeated implementation which successfully determines the optical flow for a number of image sequences.

Fleet et al. [4] proposed a new method called (phase-based optical flow). In this method, the motion detection estimates by the phase variations of the images, which leads to avoiding the disadvantages that were mentioned in the (intensity-based) method, because of that the image phase field is more robust compared with changing of the image contrast and brightness. This fact was proposed by Davis et al. [5] when they used (phase-based optical flow) method to measure the vibration modes in the cantilever beams and pipes. Also, the influence of the motion signal detection can be improved by removing the noise of the phase signal.

As a result of the mentioned researches above, it can be saying that the phase-based method has more priority with respect to (3D-DIC) and (intensity-based) methods especially in the field of micro-vibration measurements.

Chen et al. [6] presented a work that combines the motion extracting and motion magnification by using the phase-based method to extract the vibration measurement and to magnify the phase changing through the image sequence of the video, that leads to producing a new video with magnifying for the small motion. The purpose of this work is to make modal identification for simple structures like pipes and cantilever beams and also to measure the structure's vibration that was detected by the recorded video to compare the results with the traditional vibration measurement (accelerometer and laser vibrometer) results. The comparison showed that the camera results were very close to the results that were obtained by the traditional measurements. They also used the camera signal to extract the mode shapes of a simple structure and pipe. The extracted mode shapes were identical to the expected mode shape, they also produce a new video with small motion magnification. Sarrafi et al. [7] also proposed work by using the phase-based method to produce (vibration-based) structural health monitoring (SHM). In this work, the phase-based method used to extract the motion from the sequence of images (video), that was recorded by a high-speed camera, and the extracted motion information used to estimate the damage identification for a wind turbine blade. They proved that the camera can be used for structural health monitoring. However, the phase-based optical flow needs to compute the phase gradient and flow vectors, which leads to increasing the problems of noise sensitivity and time complication. Moreover, for the camera-based measurement, the quality of the captured image is very important.

The motion magnification method is a new technique that was proposed in the last few years, as a result of the fast development of the computer vision and image processing sciences in the world. It's like a microscope for the small motion because of that the small motion cannot be visible to the naked eye even when it may be having importance or effect on another application, it also may contain useful information.

Wadhwa et al. [10] presented a new Eulerian method to magnify the small motion by using the phase-based method. The motion in the images sequence (video frames) makes a local phase variation in the image frequencies. In this method, the motion detected by this local phase variation of the images sequence during the time at different scales and orientations. The phase has been determined by using the complex steerable pyramids [11]. In this method, the motion magnification is executed by magnifying the local phase difference, that caused by the small motion, this magnification will make the phase difference of the small motion equal to the same difference that caused by a bigger motion (depends on the magnification factor). As a result of this magnification, the output video will have a visible motion instead of the very small invisible motion that was existing in the raw video.

In this proposed work, (the phase-based method) technique will be used to detect the vibration signal and extract the ODS for the images sequence (video) without the need to use vibration measurements.

2. Theoretical Background

2.1. Operation Deflection Shape

As previously mentioned, every structure under an oscillation motion (vibration) must be defined by one or more points that describe the shape of the vibrated body or structure, the points called the degrees of freedom (DOFs). These points have different displacements according to the position of them with respect to the body. By collecting the deflection of many points together for one body, it will give the shape of the body under the vibration when subjected to a certain forced motion that caused the vibration, this shape called Operation Deflection Shape (ODS).

ODS is used to visualize the motion of some points in the machine structure relative to other points when the machine is running at the normal operating speed. This is different from the modal analysis where the structure is excited by an external device such as a modal hammer or shaker. ODS can be used to identify many faults. When you view the animation at the running speed of the machine you can view the motion of the bearings, potentially in three dimensions (i.e. vertical, horizontal, and axial). If a machine was out of balance, you may see a circular motion in the radial direction and minimal motion in the axial direction – unless it is an overhung machine. By looking at the axial movement you may detect misalignment, cocked bearing, or bent shaft. You can also see how the components move in relation to each other. Looking at the relative radial and axial movement, you may detect misalignment. If you study how machine components move relative to the foundations, you may detect soft foot, looseness, broken bolts, cracked welds, cracked grout, and more.

The problem detection is done by determining the time domain or frequency domain of the measured deflection. After that, the problem case can be obtained by studying the resultant data and curves of the time and frequency domains. The data must be acquired from many positions (DOFs) at the body. ODS can be used to know if the body under a resonance vibration or not by making a comparison between the operational deflection shape of the body and the mode shapes (the deflection shape at natural frequencies) of it. If the ODS is similar to the mode shape, then the body under a resonance condition.

It also can be used to detect the faults of the machines. This can be done, at first, by acquiring the data at many DOFs, like the base plate, bearing housings, motors, … etc., at the normal condition of the machine (without faults) to use them as a

reference for other conditions. After that, the data acquired for the same machine at the operating condition at the same DOFs of the normal condition. Finally, a comparison between normal condition data and operating data will be made to show if the data near or far from the normal case. The comparison is done by determining the correlation [12] coefficient between the two data. The faults can be detected by showing the correlation coefficient value for each position, if the value is high, it means that there is no fault at this position and verse versa. That makes the operation deflection shape a very good and robust tool for the machine's faults detection in the recent years.

2.2. Image Pyramids

The image pyramids are techniques in the image processing that used to change the resolution of images to be suitable for the desired applications. It is called (pyramid) because that it reduces or expands the images in a way to be like a pyramid when they arranged vertically from the base level, which represents the maximum resolution, up to the top of the pyramid, which represents the minimum resolution. Every level of the reducing process contains the half resolution of the reduced image and the verse versa for the expanding process.

The main types of pyramids that widely used in image processing are: Gaussian pyramids (the image subjects to the smoothing and spatial changing processes in both reducing and expanding pyramids) [14], and Laplacian Pyramids (It represents Gaussian high-pass filtering in addition to the resolution changing for the images) [14, 15].

Freeman and Adelson [16] proposed a new filter technique that applies to multi-scale and multi-orientation decomposition.

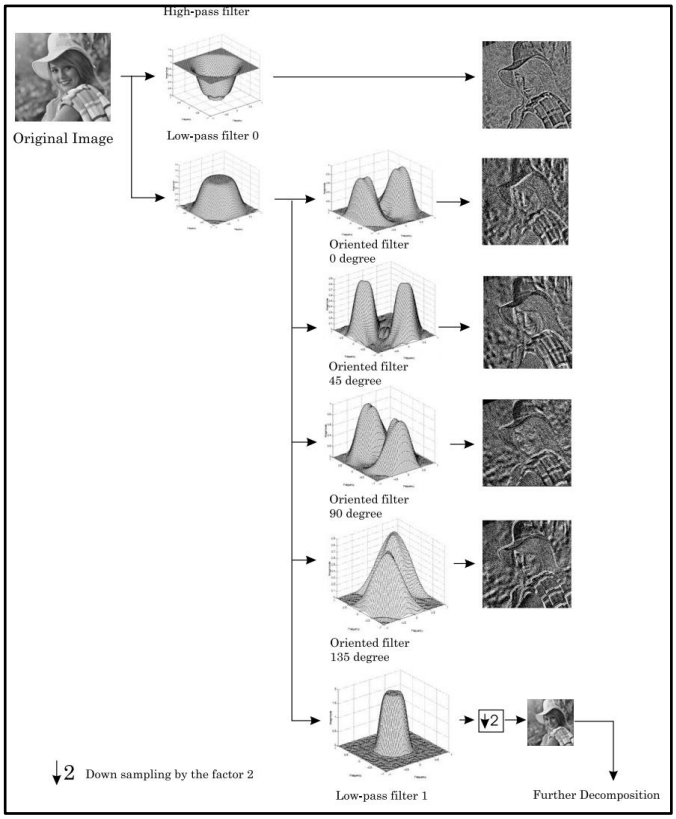

Fig. 1 Steerable pyramids decomposition [17].

By using steerable pyramids, it can be controlling the orientation of the filter in the domain because of that the filter will be a function for the orientation. Hence, it can decompose the information in the desired orientation separately, after that, it can collect all the orientation together to produce the output image with the desired enhancement.

2.3. Motion Magnification in Video

The video can be defined as a sequence of images (frames) that captured by a camera and represented sequentially with a certain speed, which depends on the camera properties. The video speed can be measured by the unit of frame per second (fps), which means the number of images that display in one second. The video can capture all the activities that occur in the real life, some of these activities are visible with the naked eye, that's mean it can be recognizing the activity or motion by eyes without using other tools like human movement, cars, and most of the other activities. There is another type of activities that they can't recognize them because they have very small motions that can't be visible with the naked eye, these motions may have very important information like the vibration in machines, these reasons give a motivation to propose techniques to magnify this small motion to make it visible. Many techniques have been introduced in the field of video motion magnification.

2.4. Phase-Based Motion Magnification

As previously mentioned, there are two methods for motion magnification: Eulerian and Lagrangian methods. Eulerian method is useful in small motion magnification techniques because it depends on the principle of decomposing separately every frame in the video instead of processing every pixel in the frame, as the principle of work for the Lagrangian method. The frames will subject to temporal processing to detect the motion in the frames sequence (video).

Every image contains data for the intensity value of each pixel. It can be supposing the intensity is a 1-D function that can be expressed as $I(x, t)$, which represent the image intensity at spatial position x and time t. The motion will produce intensity changing, it can be representing the motion by the intensity function. The intensity at (t = 0) is $I(x, t) = f(x)$, and at t is:

$$I(x, t) = f\left(x + \delta(t)\right) \tag{1}$$

where $\delta(t)$ represents a displacement function that refers to the motion. The magnification process can be applying by multiply $\delta(t)$ with $(1 + \alpha)$, as the expression below:

$$\hat{I}(x, t) = f\left(x + (1 + \alpha)\,\delta(t)\right) \tag{2}$$

where α is the magnification factor. This equation is the goal of every motion magnification type, where $\hat{I}(x, t)$ represents the resultant intensity of the magnified image. Many works, that deal with Eulerian method, have been proposed .

(Phase-Based Motion Magnification) is one of the techniques of Eulerian motion magnification. It relies on representing the function of image intensity $f(x)$ as a Fourier series. That leads to determine the intensity function of the subtle motion $f(x + \delta(t))$ according to the expression [10]:

$$f\left(x+\delta(t)\right)=\sum_{\omega=-\infty}^{\infty} A_{\omega}\, e^{\,i\omega\,(x+\delta(t))} \tag{3}$$

where A_ω represents the intensity amplitude. In this method, the magnification applies to the frequency phase instead of the amplitude, that occurred in the first-order method [9].

The first step is the computation of the local phase of function f for every spatial scale and orientation by using the steerable pyramid. After that, the function applies to a band-pass filter for extract the desired frequency ω, the frequency band of ω is [10]:

$$S_{\omega}(x,t)=A_{\omega}\, e^{\,i\omega\,(x+\delta(t))} \tag{4}$$

The phase $\omega\,(x+\delta(t))$ contains the information of motion because S_ω is sinusoid. Therefore, the phase will be extracting and filtering to remove $\omega\, x$ component [10], the result of this process is:

$$B_{\omega}(x,t)=\omega\,\delta(t) \tag{5}$$

Finally, the magnification process applies on B_ω by multiplying it by the magnification factor α, and adding the results to the phase of S_ω to introduce the output of magnified process by the expression [10]:

$$\hat{S}_{\omega}(x,t)=S_{\omega}(x,t)\; e^{i\alpha B_{\omega}}=A_{\omega}\; e^{i\omega\,(x+(1+\alpha)\,\delta(t))} \tag{6}$$

The phase-based method overcomes the disadvantages that were found in the first-order method. The main priority is that the magnification process similar to the true magnification that needs to determine it because the true motion causes a difference in the phase of function f . Therefore, when the phase difference (that caused by a subtle motion) magnifying, the subtle motion will directly be magnified and look like a true large motion in the output video instead of the intensity magnifying that occurred in the first-order method [9]. It also has the advantage of the noise, which will only be translated instead of the noise magnification in the first-order method. The magnification limit in the phase-based method is also larger than the first-order method. It was determined as [10]:

$$\alpha\,\delta(t)<\frac{\lambda}{4} \tag{7}$$

That gives more priority to this method to use it in the applications that have a motion with high frequencies and a small wavelength. For all of these advantages of this method, it will be used to magnify the subtle motion that was occurring as a result of the vibration in the structures and rotating machines. The magnified video can represent a simulation of the operating deflection shape (ODS) for the equipment, instead of using engineering programs that are complicated and take a long time to execute the simulation.

Figure 1 explains the difference between first-order and phase-based motion magnification methods. It shows that the phase-based method has more agreement with the true motion magnification, which gives the phase-based method more priority.

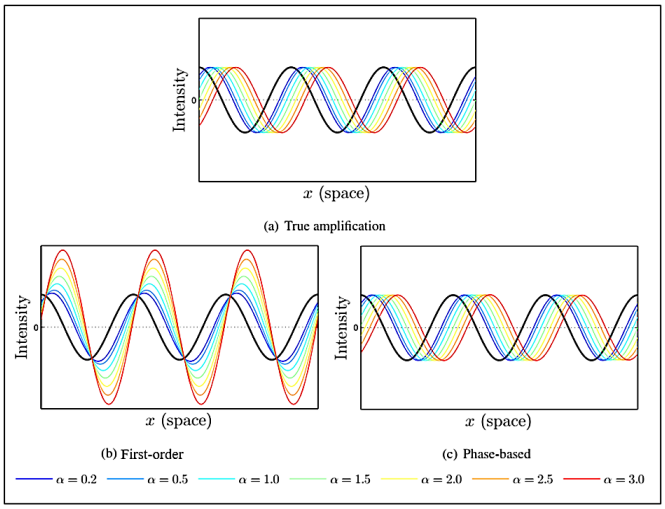

Fig. 2 The Comparison between the motion magnification methods with true motion magnification [10].

2.5. Vibration Extraction from Video

Every video consists of frames (images) sequence, and every video contains a finite number of frames that are displayed at a certain speed which is measured by frame per second (fps). Each video frames contain a finite number of pixels, which depends on the camera specifications that have been used to record the video, the pixels value represents the image information and they differ from frame to another.

The pixel's value can be introduced as a 1D or 2D function. The motion can be sensed by the change in the pixels value function for each video frame. The small motion of vibration just causes a very small and oscillation changing in the image content, which makes the function only shifted in a certain direction without changing for its values. Therefore, this fact can be represented, the phase changing of pixels function, as an indication for vibration measuring to the objects that were captured in the recorded video. Peng et al. [13] derived a mathematical expression that can calculate the vibration displacement from the phase difference, the expression is:

$$\Delta x=\lambda * \frac{\varphi\left(I\,(x,t+\Delta t)\right)-\varphi\left(I\,(x,t)\right)}{2\pi} \tag{8}$$

where Δx is the displacement, λ is dimension unit to pixel ratio ((dimension unit) / pixel), and φ is the function phase. From Eq. (8), it can be concluding that the displacement is proportional to the phase difference, that conclusion leads to present a new and very useful method for the non-contact vibration measurement. Dimension to pixel ratio λ must be calculated separately for every recorded video because it depends on the focal length of the camera and the distance between the camera and the vibrated object. This calculation can be represented as a camera calibration. The calibration can be accomplished by taking a photo for a known-dimensions object or spot, the pixels number that represented this object can be calculated. After that, the object dimension divides by the calculated pixels. The calibration object and the vibrated body must be at the same position (the same distance from the camera) to get the exact dimension to the pixel ratio. The location of the camera should not change at both the calibration and recording processes.

3. Experimental Work

3.1. High-Speed Camera

To measure the vibration for an object, sensors must be used. As mentioned in the last chapters, there are two types of vibration measurements, contact, and non-contact measurements. A high-speed camera can be used as a non-contact measurement. The main difference between the high-speed camera and other camera types is that it records a video with a high frame rate (frames per second or fps), which means the recorded video consist of a very large number of frames for every second. That leads to get more information about the object that was captured in the video, essentially when the object is moving at a small motion with very high speed like the machine under vibration.

This camera feature (high fps) can be exploited because the large number of fps means very large information about objects or equipment, especially when the resolution is also high. In other words, when the camera is used as a vibration measurement, fps can be represented as the sampling rate of the camera. Therefore, the higher fps number, the better representation for vibration signals and the wider range of frequencies that can be detected. That means when a camera is to be used for vibration measurement applications, camera fps must be checked if it is suitable for the working speed of application and the expected faults that wanted to be detected and their signal analysis.

In this work, a high-speed camera (FLIR Blackfly S BFS-U3-23S3C) that shown in Fig. 3 (a) has been used, Table 1 shows the main camera specifications with a lens (FUJINON HF25HA-1S) as shown in Fig. 3 (b).

Table 1 Camera specifications.

Property	Specifications
Model	FLIR Blackfly S BFS-U3-23S3C
Maximum Resolution	1920 × 1200
Frame Rate at (Max. Resolution)	163 fps
Megapixels	2.3 MP
Chroma	Color

Fig. 3 (a) FLIR high-speed camera, (b) FUJINON camera lens.

The camera options (fps, resolution, exposure time, … etc.) can be controlled by the camera software that downloaded from FLIR website. The software is very important to control the acquisition options that will be affected on the recorded video, which, in turn, will be directly affected on the signal that will be taken from the video. For this reason, the software must be checked carefully to get clear data with good precision.

3.2. Verification Test Setup

To get an experimental approval for using a high-speed camera as a vibration measurement device, a verification test must be done. In this test, the vibration must be detected by the camera and another sensor, which must be commonly used for vibration detection. The test has been accomplished by using the machinery faults simulator, proximity sensor, and high-speed camera. The camera has been connected to a laptop by a USB cable to run the camera software and record the desired video. Fig. 4 and 5 show the experimental setup for this test.

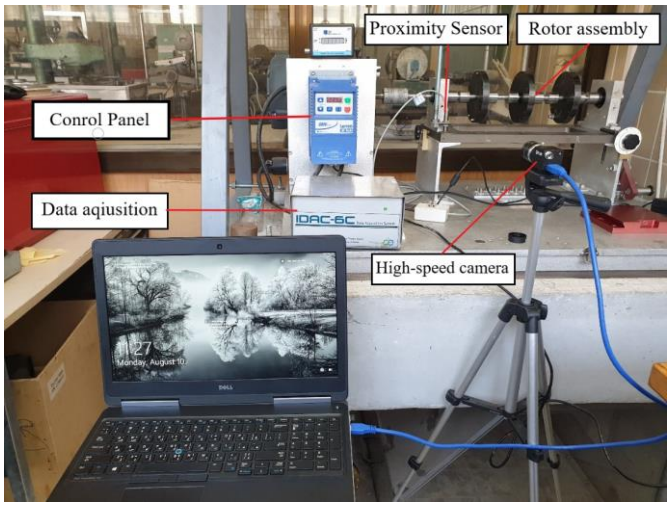

Fig. 4 Experimental setup for the verification test.

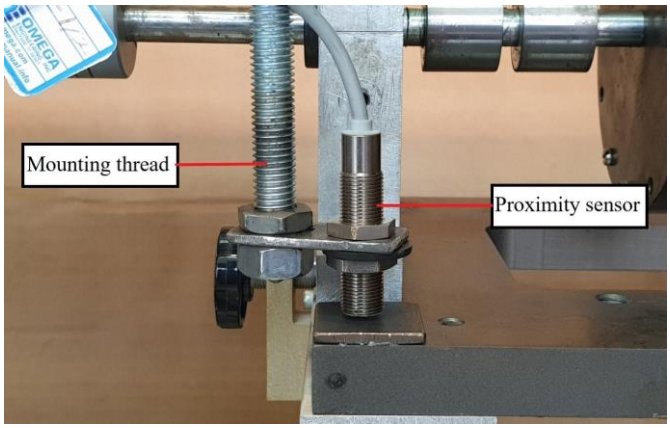

Fig. 5 proximity setup for the verification test.

The camera must be at the same level of the measured point to sense the exact displacement of the desired point in a certain direction in the picture plane. Therefore, the camera mounted by a tripod to easily adjust the level and angle of the camera. The camera has been set to record a video with properties shown in Table 2. The properties of the camera were set by using the software after the camera has been connected to the laptop.

Table 2 The properties of verification test video.

Property	Value
Time	2.56 sec
Frame rate	200 fps
Video frames	512
Width	1080 pixel
Height	720 pixel

The machinery faults simulator has been operated with a rotor, which is shown in Fig 4. An unbalance mass (16.5 gram) has been added, the rotating speed was (20 Hz or 1200 rpm). The left bolt of the foundation support has been removed to make a looseness fault. The proximity sensor was mounted by using a long thread, that was attached to the simulator structure, in a way to measure the foundation vibration. The proximity sample rate was 2048 Hz. In this test, the vibration data, that has been extracted from the recorded video, compared to the data that was acquired by the proximity sensor. To get the verification purpose, the two compared signals must be very close to each other to prove that the camera can be used as a non-contact vibration measurement device.

3.3. Mode Shapes Tests Setup

Mode shapes of a system appear when the system is operating at its natural frequencies. Therefore, a system that operates at the natural frequencies must be used to study the operation deflection shape at the natural frequencies. In this work, the whirling of shafts apparatus (Fig. 6) has been used to accomplish the test. The camera has been used to measure the displacement of the shaft and detect the operational deflection shape at the first and second modes. The phase difference will be calculated between any two points on the shaft to prove that the shaft at a certain mode shape, depending on the value of phase difference, that will make this method (use a camera as a vibration measurement) more robust.

The positions of the points have been selected according to the expected mode shape at the operating speed. While the whirling shaft apparatus used, the mode shape is easily predictable because it can be clearly seen. The experimental setup of this test as shown in Fig. 7.

Fig. 6 Whirling of shaft apparatus.

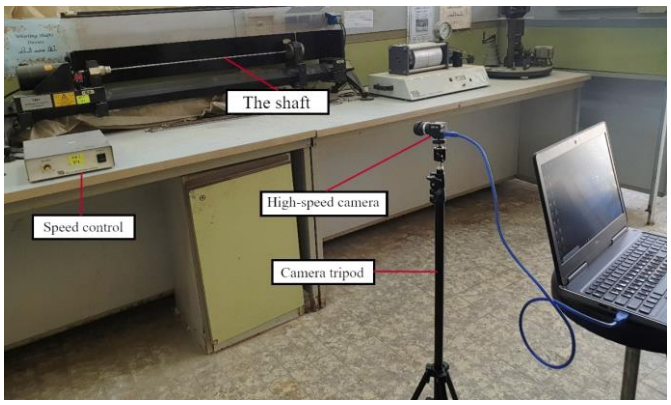

Fig. 7 Experimental setup for Mode Shapes test.

The camera has been installed in a position to get a video that will cover all the shaft length. It has been used to record two videos at two rotating speeds, which represent the first and second natural frequencies of the used shaft. The properties of the recorded videos are described in Table 3.

Table 3 The properties of (Mode Shapes tests) videos.

Property	Value
Time	2.56 sec
Frame rate	200 fps
Video frames	512
Width	1920 pixel
Height	300 pixel

The shaft length is (0.9 m) with a diameter (7 mm). It was supported by a (hinged-hinged) method. The test has been carried out by gradually increasing the rotating speed of the shaft until reached to the first mode shape at the first natural frequency, which was equal to (1080 r.p.m. or 18 Hz). The first mode shape was clearly shown and recognized. At this speed, the video has been recorded to get the vibration data for the shaft in the first mode shape. From this data, the operation deflection shape will be measured and displayed by the designed program, that will be discussed in the next section, the phase difference will be also calculated between many points to prove that the shaft at the first mode shape.

After that, the speed was gradually increased until reached to the second critical speed, which was equal to (3600 r.p.m. or 60 Hz). The same steps that were mentioned in the first mode shape have been repeated in the second mode. The operation deflection shape and phase difference will also be calculated at this mode to show that the camera is a good and robust device for vibration measurement and it can be used to detect the mode shapes of objects.

4. Results and Discussion

4.1. Verification Test Results

As mentioned, for the verification test, a proximity sensor and high-speed camera have been used. At first, the camera calibration must be accomplished. The calibration has been done by taking a photo for a measuring tape because it has visible known-dimensions, as shown in Fig. 8.

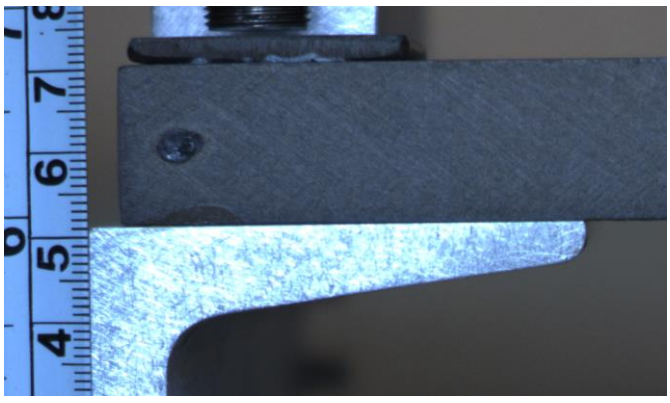

Fig. 8 The camera calibration image.

The pixels number between two points on the measuring tape has been calculated. After that, the real dimension between the selected points divided by the number of the pixels that have been calculated. All these calibration procedures have been executed by using the designed program at (Vibration Detection GUI window). The sampling rate of the sensor was (2048 Hz), while the camera was set to record a video with (200 fps). It was difficult to acquire the data for both devices at the same time because of that every device (camera and sensor) has special software for data acquisition, that led to restricting the comparison process.

For this reason, the comparison has been accomplished by calculating RMS value and maximum peak value for the time domain at each device, the obtained frequencies in the FFT figures are also computed for each reading. After that, the error percentage for the values was calculated by the expression below:

$$Error\ \% = \frac{|S_r - V_r|}{S_r} \times 100\ \% \quad (9)$$

Where *Sr* is the sensor readings and *Vr* is the video readings.

The machine fault simulator has been operated at a speed of (20 Hz) with a looseness fault in the driven end foundation. The figures of the time and frequency domains were plotted for each reading. The RMS value and maximum peak value have been extracted from the time domains. According to these values, the error percentages have been calculated. The error percentage for the obtained frequencies in the FFT domain at each device also calculated. Table 4 shows the values of the calculated error percentages. This high value may be attributed to that the signals not acquired at the same time for both proximity sensor and high-speed camera, it also may be attributed to the camera calibration process because of that the two pixels, that was selected to execute the calibration, have been roughly selected at the exact position on the picture. It also, in the Table 4, can be showing that the error percentages values of the maximum obtained frequencies in the FFT domain are very low, which means that the obtained frequencies by the camera signal are very identical to the frequencies that were obtained by the proximity sensor. From the results above, the verification test presents reasonable validation that the displacement extracted from a recorded video is mostly accurate and that the operational deflection shapes and the phase difference of any object can be successfully measured by using a high-speed camera.

Table 4 The error percentages of the verification test.

The Property	Proximity Sensor	Camera	Error (%)
Displacement RMS Value (mm)	0.0126	0.0121	3.9 %
Maximum Peak Value of Displacement (mm)	0.02448	0.02888	17.9 %
1st Frequency in FFT (Hz)	20	19.91	0.45 %
1st Frequency Amplitude (mm)	0.016	0.015	6.25 %
2nd Frequency in FFT (Hz)	40	39.82	0.45 %

Figs. 9-12 show the time and frequency domains for both the proximity and high-speed camera. They also contain the values that were used to make the desired calculations above.

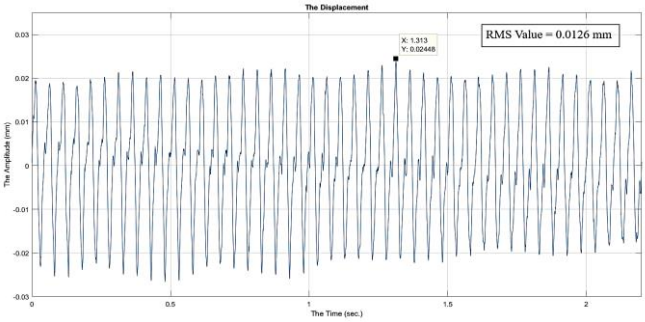

Fig. 9 Time-domain of proximity displacement signal.

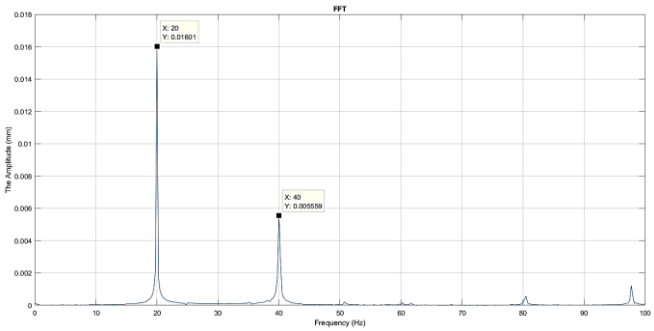

Fig. 10 Frequency domain of proximity displacement signal.

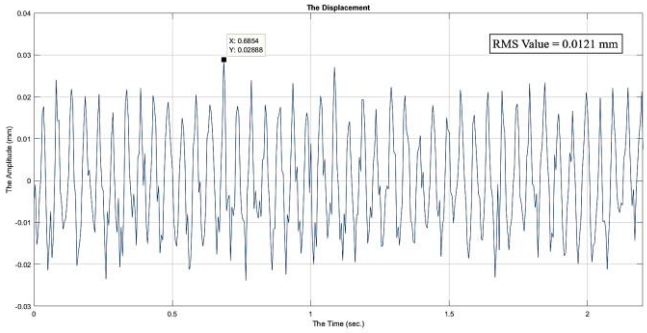

Fig. 11 Time-domain of camera displacement signal.

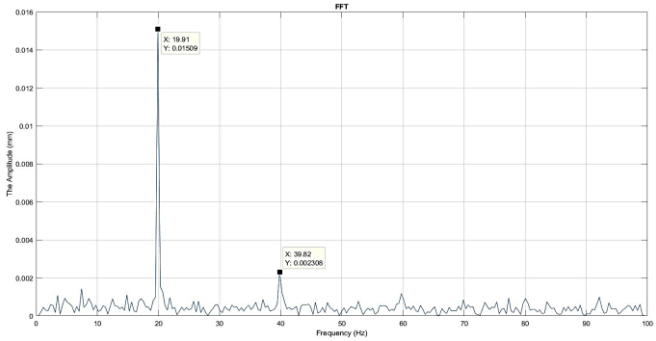

Fig. 12 Frequency domain of camera displacement signal.

4.2. Results of Mode Shapes Tests

4.2.1. First Mode Shape

The test has been executed by using the whirling of shaft apparatus, as mentioned in the last chapter. The speed was gradually increased until reaching to the experimental first mode shape at a speed of (18 Hz). At this speed, the camera has been used to record the video. By using the designed software, the video was processed to select 3 points on the rotating shaft to measure the vibration signals of the shaft, as

shown in Fig. 13 below, which will be used to obtain the operation defection shape at the first natural frequency (first mode shape).

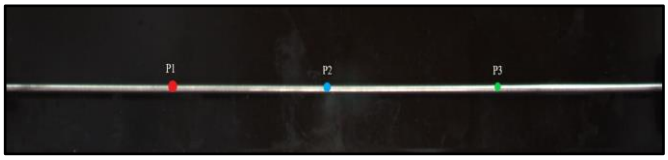

Fig. 13 Selected points positions of (mode 1) video.

The signals also used to calculate the phase differences between the points to check if the camera signal can be used to prove that the shaft under a certain mode. Figs. 14-16 show the time and frequency domains for the selected points. From the figures, it can be shown that the obtained frequency (17.96 Hz) closely identical to the expected frequency, which is equal to the operating speed (18 Hz). It also can be showing that the position of the maximum displacement was at (P2), which is in the middle of the shaft, this position is identical to the expected position of the maximum displacement when the shaft rotates at (1st mode).

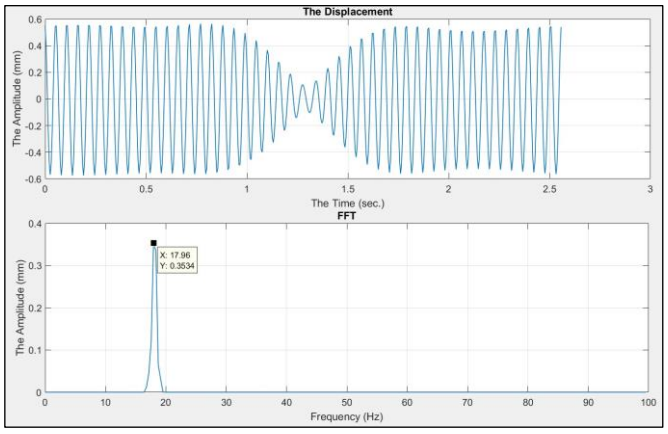

Fig. 14 Time and frequency domain of (mode 1-P1).

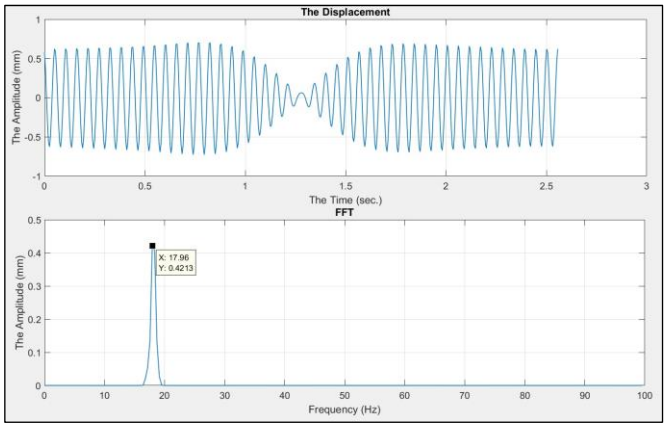

Fig. 15 Time and frequency domain of (mode 1-P2).

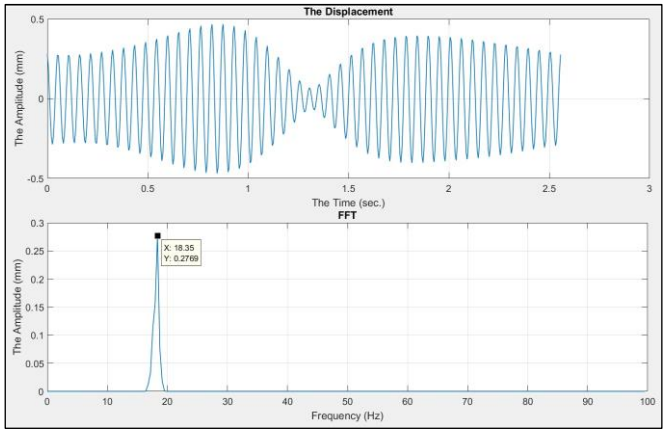

Fig. 16 Time and frequency domain of (mode 1-P3).

Figure 17 shows the extracted operation deflection shape (ODS) of the shaft for 7 sequential frames, which represents the (ODS) of every shaft cycle at (1st mode).

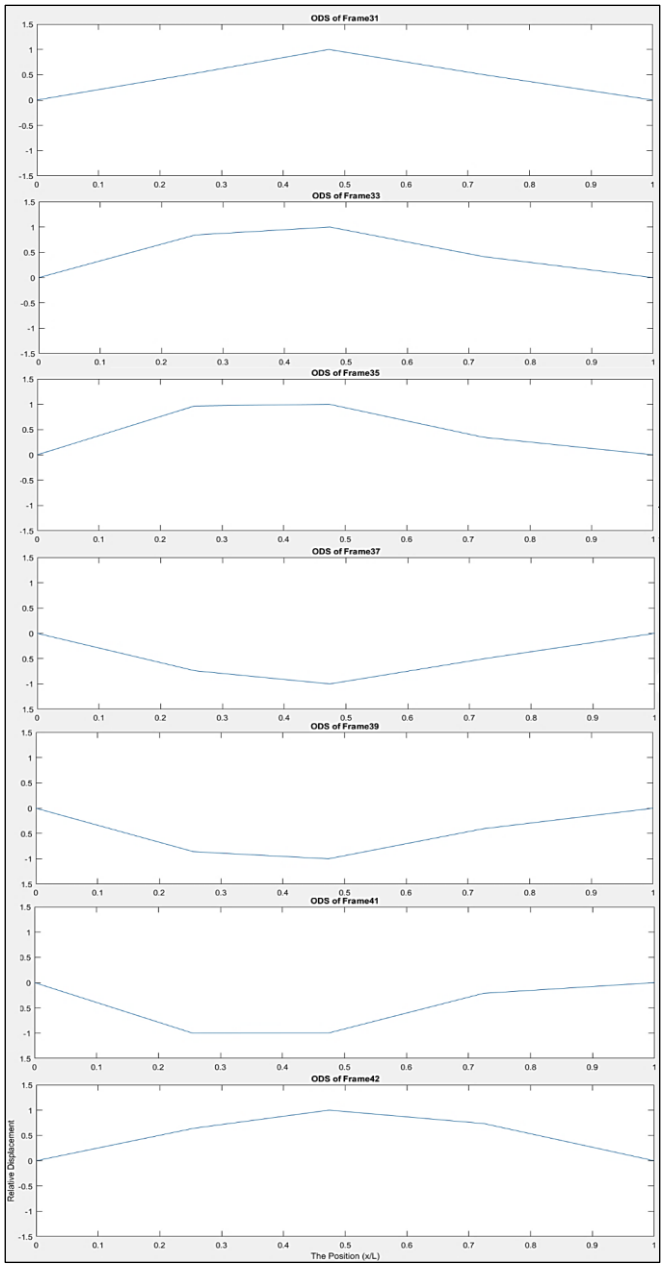

Fig. 17 The extracted operation deflection shape at (1st mode).

The X-axis represents the point position with respect to the shaft length, while Y-axis represents the relative displacement with respect to the maximum displacement at the frame. the extracted ODS is very identical to the ODS that was shown by the eyes when the test was accomplished.

The phase differences also have been extracted. The designed software contains special components in (Results GUI window) that are used to calculate the phase difference between any two selected points by using (cross power spectral density) function for the frequencies which they under the Nyquist frequency. It must be focusing on the frequency of the extracted mode shape to calculate the phase difference between the points signals. Fig. 18-20 show the phase difference between P1-P2, P1-P3, and P2-P3 respectively. The figures show that all the points are mostly in phase, this result agrees with the extracted ODS.

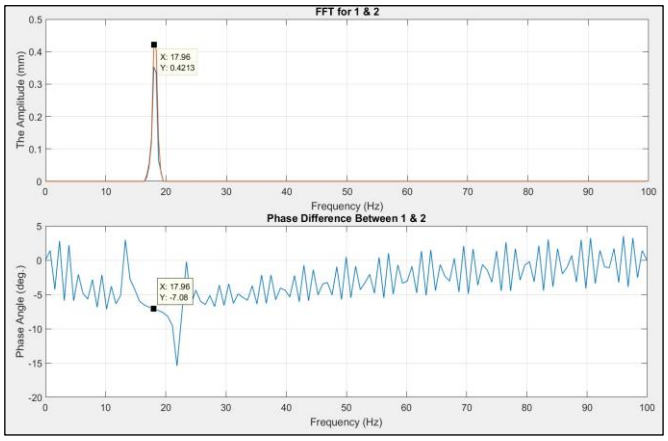

Fig. 18 The phase difference between (P1- P2) in mode 1.

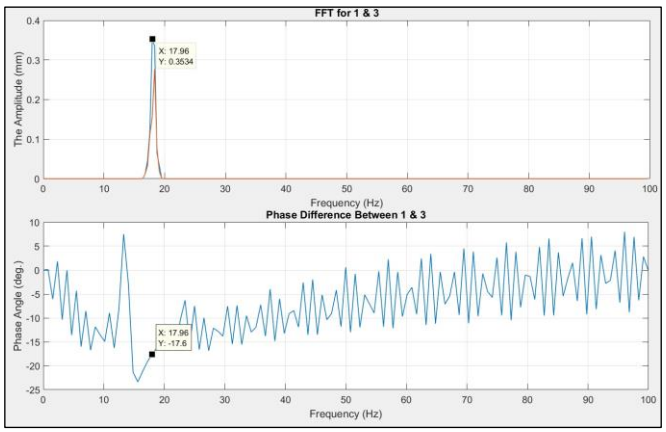

Fig. 19 The phase difference between (P1-P3) in mode 1.

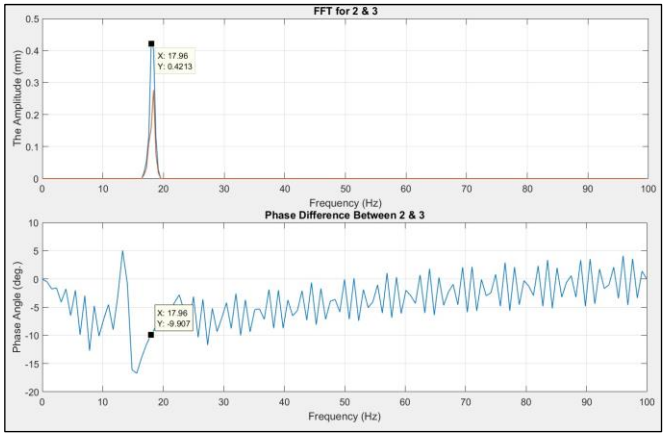

Fig. 20 The phase difference between (P2-P3) in mode 1.

4.2.2. Second Mode Shape

After recording the video of the first mode, the speed was gradually increased until reached to the experimental second mode shape at a speed of (60 Hz). At this speed, the camera has been used to record the video. By using the designed software, the video was processed to select 6 points on the rotating shaft to measure the vibration signal of the shaft, as shown in Fig. 23 below, which will be used to obtain the operation defection shape at the second natural frequency (second mode shape).

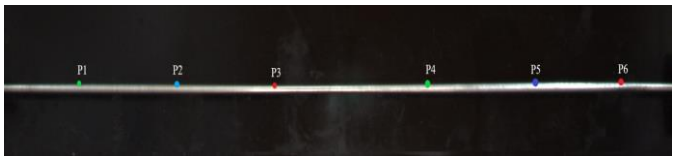

Fig. 21 Selected points positions of (mode 2) video.

The positions of points have been selected according to the expected mode shape in the second mode. the number of points also must be suitable to get a good representation for the operation deflection shape of the shaft in the second mode. Figs. 22-27 show the time and frequency domains of the selected points. From the figures, it can be shown that the obtained frequency (60.12 Hz) closely identical to the expected frequency, which is equal to the operating speed (60 Hz). It also can be showing that the position of the maximum displacement was at (P2) and (P5), which is also identical to the expected position of the maximum displacement when the shaft rotates at (mode 2).

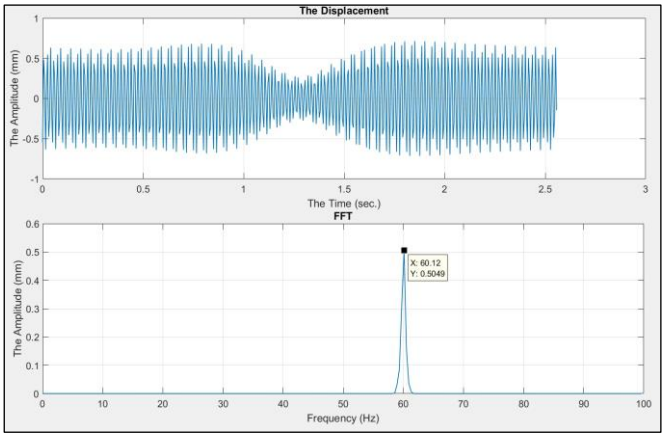

Fig. 22 Time and frequency domain of (mode 2-P1).

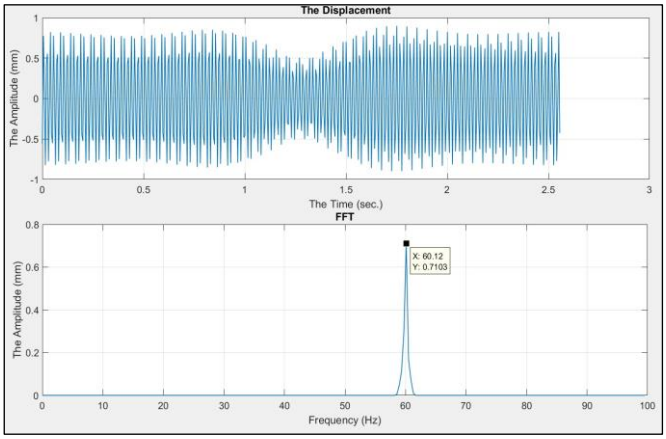

Fig. 23 Time and frequency domain of (mode 2-P2).

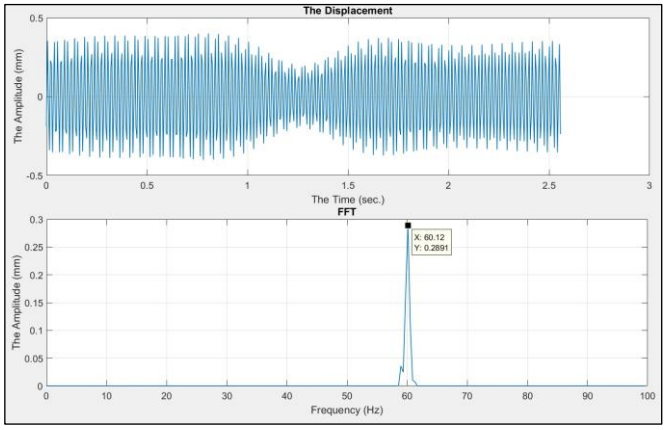

Fig. 24 Time and frequency domain of (mode 2-P3).

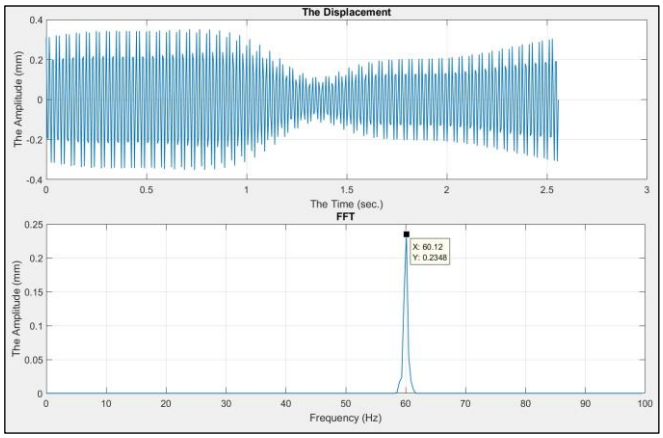

Fig. 25 Time and frequency domain of (mode 2-P4).

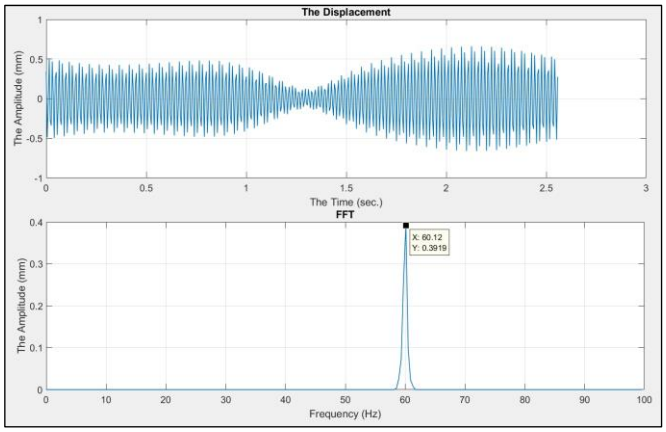

Fig. 26 Time and frequency domain of (mode 2-P5).

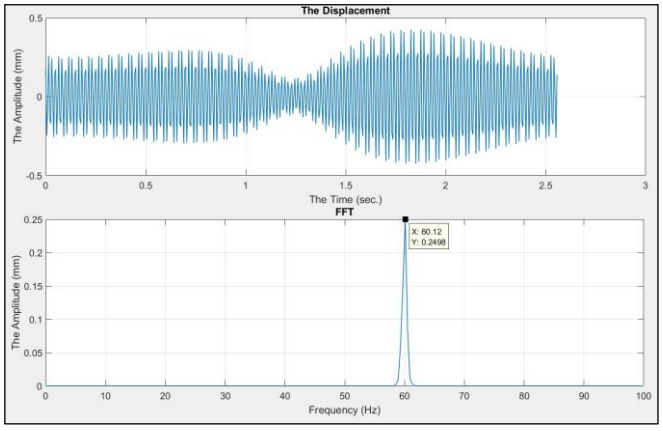

Fig. 27 Time and frequency domain of (mode 2-P6).

Figure 28 shows the extracted operation deflection shape (ODS) of the shaft for 7 sequential frames, which represents the (ODS) of every shaft cycle at (mode 2). From Fig. 30, it can be shown that the extracted (ODS) is very identical to the ODS that was showed and expected when the shaft rotates at mode 2.

The phase difference at mode 2 has been extracted. As it was previously done in mode 1, it must be focusing on the mode shape frequency to determine the phase difference between certain points. In this test, the phase difference between (P2-P5) has been extracted because, at mode 2, the phase difference between these points must be equal or near to (180 deg.) out of phase, as shown in Fig. 29. From Fig. 29, it can show that the phase difference between (P2-P5) at the frequency of (60.12 Hz) is (178.5 deg.) out of phase, which is very close to the expected value (180 deg.). The result is also mostly identical to the extracted ODS.

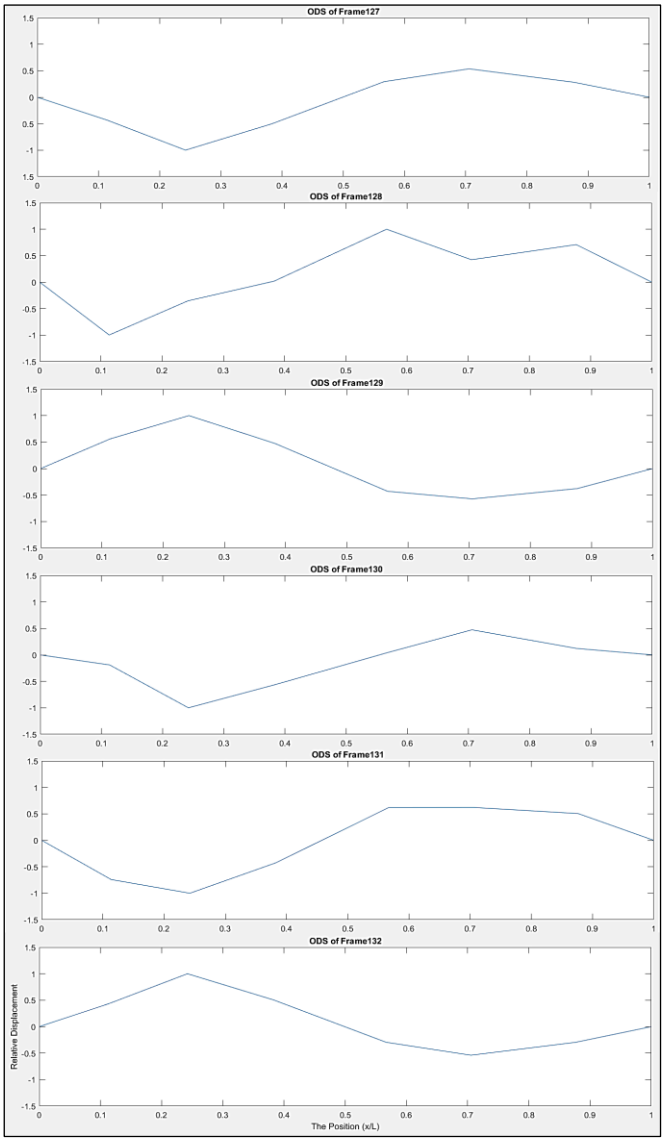

Fig. 28 The extracted operation deflection shape at (2nd mode).

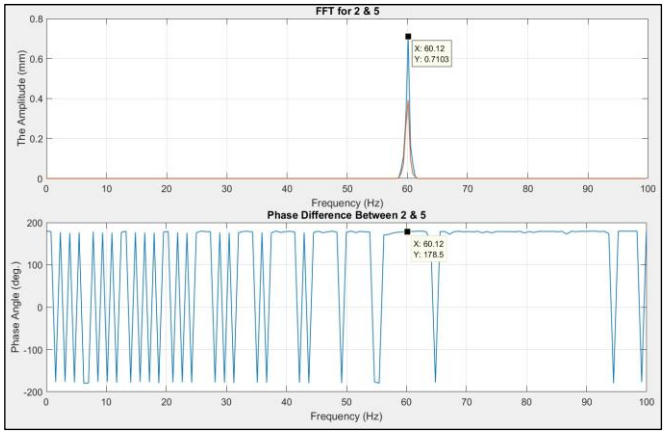

Fig. 29 The phase difference between (P2-P5) in mode 2.

5. Conclusions

From this proposed work and the discussions that were previously presented, it can get some conclusions. At first, the verification results proved that the frequencies that extracted by the camera were agreed with the frequencies that were extracted by the proximity sensor by (99.55 %). They also proved that the error percentage of the displacement RMS value was (3.9 %). From these results, the verification test presents reasonable validation that the operational deflection shapes and the phase difference of any object can be successfully measured by using a high-speed camera. The high error percentages of the compared amplitudes may be referring to that the data acquisition process was not be taken at the same time because we didn't have a software that acquires the data for both camera and proximity at the same time.

From the mode shape tests, the high-speed camera can be used to detect the operation deflection shapes and the phase angle difference between the selected points on a rotating shaft. This conclusion has been proved by the obtained results which were shown that the extracted ODS at the first two critical speeds was clearly identical to the expected ODS, which they are already known for the rotating shaft at its critical speeds. The results also showed that the extracted phase difference between certain points was closely identical to the expected phase difference at these points when the shaft operates at the critical speeds.

To acquire a clear and more accurate signal from a recorded video, the selected points most be very close to the edges of the vibrated object that was captured in the video. The video background also must be at one color, the background color must be chosen in a way that makes the object edges clearly recognized.

References

[1] Ziyi Zhang, Pingyu Zhu, and Xiaoyi Bao, "The mass loading effect on lightweight cantilever mode frequency measurement by optical fiber sensor", Proceedings of Photonics North 2008, Event for Society of Photo-Optical Instrumentation Engineers (SPIE), Vol. 7099, pp. 1-10, 2008.

[2] Mark N. Helfrick, Christopher Niezrecki, Peter Avitabile and Timothy Schmidt, "3D Digital Image Correlation Methods for Full-field Vibration Measurement", Elsevier, Mechanical Systems and Signal Processing, Vol. 25, No. 3, pp. 917-927, 2011.

[3] Berthold K. P. Horn and Brian G. Schunck, "Determining Optical Flow", Proc. SPIE, Techniques and Applications of Image Understanding, Vol. 0281, 1981.

[4] D. Fleet and Y. Weiss, Optical Flow Estimation, Handbook of Mathematical Models in Computer Vision for Springer, pp. 237-257, 2006.

[5] Abe Davis, Katherine L. Bouman, Justin G. Chen, Michael Rubinstein, Frédo Durand and William T. Freeman, "Visual Vibrometry: Estimating Material Properties from Small Motion in Video", IEEE Conference on Computer Vision and Pattern Recognition (CVPR), pp. 5335-5343, 2015.

[6] Justin G. Chen, Neal Wadhwa, Young-Jin Cha, Frédo Durand, William T. Freeman and Oral Buyukozturk, "Modal identification of simple structures with high-speed video using motion magnification", Elsevier, Journal of Sound and Vibration, Vol. 345, pp. 58-71, 2015.

[7] Aral Sarrafi, Zhu Mao, Christopher Niezrecki and Peyman Poozesh, "Vibration-based damage detection in wind turbine blades using Phase-based Motion Estimation and motion magnification", Elsevier, Journal of Sound and Vibration, Vol. 421, pp. 300-318, 2018.

[8] Ce Liu, Antonio Torralba, William T. Freeman, Frédo Durand, and Edward H. Adelson, "Motion Magnification", ACM Transactions on Graphics (TOG), Vol. 24, No. 3, pp. 519-526, 2005.

[9] Hao-Yu Wu, Michael Rubinstein, Eugene Shih, John Guttag, Fredo Durand, William Freeman, "Eulerian Video Magnification for Revealing Subtle Changes in the World", ACM Transactions on Graphics (TOG), Vol. 31, No. 4, 2012.

[10] Neal Wadhwa, Michael Rubinstein, Frédo Durand and William T. Freeman, "Phase-Based Video Motion Processing", ACM Transactions on Graphics (TOG), Vol. 32, No. 4, 2013.

[11] W. T. Freeman and E. T. Adelson, "The Design and Use of Steerable Filters", IEEE Transactions on Pattern Analysis and Machine Intelligence, Vol. 13, No. 9, pp. 891-906, 1991.

[12] D. J. Ewins, "Modal Testing: Theory, Practice and Application", Research Studies Press LTD, Second edition, 2000.

[13] Cong Peng, Cong Zeng and Yangang Wang, "Camera-Based Micro-Vibration Measurement for Lightweight Structure Using an Improved Phase-Based Motion Extraction", IEEE Sensors Journal, Vol. 20, No. 5, pp. 2590-2599, 2020.

[14] E. H. Adelson, C. H. Anderson, J. R. Bergen, P. J. Burt and J. M. Ogden, "Pyramid Methods in Image Processing", RCA engineer, Vol. 29, No. 6, pp. 33-41, 1984.

[15] Peter Burt and Edward Adelson, "The Laplacian pyramid as a compact image code", IEEE Transactions on communications, Vol. 31, No. 4, pp. 532-540, 1983.

[16] W. T. Freeman and E. T. Adelson, "The Design and Use of Steerable Filters", IEEE Transactions on Pattern Analysis and Machine Intelligence, Vol. 13, No. 9, pp. 891-906, 1991.

Biographies

Jaafar Khalaf Alsalaet received M.Sc. and Ph.D. Degrees from Department of Mechanical Engineering, College of Engineering, University of Basrah, Iraq in 1998 and 2012 respectively. Worked as consultant to many industrial foundations in the field of vibration analysis, machinery diagnosis and dynamic balancing. Worked in the design and implementation of many measurement and control instruments since 1998 including portable vibration measurement and analysis systems, dynamic balancing upgrade instrument, speed and temperature control and other devices. Worked as assistant professor in the department of mechanical engineering since 2017. Have published many papers in vibration analysis and boundary element methods in 3D elastodynamic problems.

Husam Sattar Jasim received his B.Sc. degree in Mechanical Engineering from the Department of Mechanical Engineering, College of Engineering, University of Basrah, Iraq in 2013. He is currently pursuing an M.Sc. degree in Mechanical Engineering.